PHYSICAL REVIEW E **72**, 065301(R) (2005)

Determining the spectral signature of spatial coherent structures in an open cavity flow

L. R. Pastur, F. Lusseyran, Y. Fraigneau, and B. Podvin
LIMSI, University of Paris XI, 91403 Orsay Cedex, France
(Received 28 July 2005; published 12 December 2005)

We applied to an open flow a proper orthogonal decomposition (POD) technique, on two-dimensional (2D) snapshots of the instantaneous velocity field, to reveal the spatial coherent structures responsible for the self-sustained oscillations observed in the spectral distribution of time series. We applied the technique to 2D planes out of three-dimensional (3D) direct numerical simulations on an open cavity flow. The process can easily be implemented on usual personal computers, and might bring deep insights regarding the relation between spatial events and temporal signature in (both numerical or experimental) open flows.

DOI: 10.1103/PhysRevE.72.065301 PACS number(s): 47.15.Ki, 07.05.Kf, 07.05.Pj, 05.45.Tp

One of the most challenging questions arising in open flows such as jets, mixing layers, etc., is to understand the occurrence and nature of robust and reproducible self-sustained oscillations revealed in spatially localized time series, usually velocity, or pressure measurements. How such frequencies appear, and whether or not they might be the signature of particular coherent spatial patterns, still remain largely unresolved, although abundantly documented [1,2]. Such an understanding may, moreover, appear of the utmost importance in control applications, in that knowing which spatial event is generating such spectral signature may lead to the best-fitted control scheme with respect to the required goal. An example is given by flows over open cavities, as in high-speed trains, that generate very powerful self-sustained oscillations that appear to be the main source of noise emitted by the train. In that case, control will be aimed to reduce or even suppress the source of noise, without reducing the aerodynamic performances, and at the lowest energetic cost.

In this paper we (i) show in a test case the ability of the proper orthogonal decomposition (POD) technique to associate self-sustained oscillations to well-identified spatial coherent structures; (ii) confirm, as a consequence, the mixing layer origin of the most energetic self-sustained oscillations in an open cavity flow. We will show that two-dimensional (2D) cuts out of the fully three-dimensional (3D) flow are sufficient to extract significant space-time events out of the flow. We are using for that purpose a technique based on an empirical decomposition of the flow that optimizes a basis of (orthogonal) eigenmodes with respect to the kinetic energy. The technique is often known as the proper orthogonal decomposition in the framework of fluid dynamics [3,4], or as the Karhunen–Loève decomposition in the framework of signal processing [5]. (Other denominations exist, such as empirical orthogonal decomposition, singular value decomposition, etc., depending on the field of application considered.) To illustrate our point, we applied the technique to 3D direct numerical simulations of an air flow over an open cavity [6]. The system is a cavity of length $L=10$ cm along x (the longitudinal direction along which air is flowing), of depth $h=5$ cm (the aspect ratio L/h is 2), and transverse size $l=20$ cm. The cavity is enclosed in a vein 12 cm high. The flow-rate velocity is $U_0=1.2$ m/s (Reynold's number $\mathrm{Re}\simeq 8500$). Simulations were performed following a finite-volume approach under an incompressible flow hypothesis. Spatial and time discretization have a second-order precision. The pressure field is given by a Poisson's equation that requires a projection step, in order to be in agreement with a nondivergent velocity field. In order to reduce the CPU time cost, the spanwise boundary conditions are periodic. The $256\times128\times128$ mesh-spatial grid is refined in areas featuring strong velocity gradients (boundary and shear layers)—with a mesh varying from 0.7 to 10 mm along the longitudinal x and vertical y directions, and constant with about 1.56 mm over the transverse direction z [7]. The input boundary layer is of Blasius type (velocity profile solution of the simulations).

Here we briefly expose the POD technique we implemented. The goal is to compute the eigenmodes $\{\phi_n(t),\vec{\psi}_n(\vec{r})\}$ that best fit the coherent structures composing the flow, computed from a database of M different snapshots of the velocity field, in such a way that any instantaneous snapshot of the database can be reconstructed by performing the sum over the eigenmode basis,

$$\vec{u}(\vec{r},t)=\sum_{n=1}^{M}\mu_n\phi_n(t)\vec{\psi}_n(\vec{r}), \tag{1}$$

where $\lambda_n=\mu_n^2$ are the eigenvalues of the decomposition [3]. Typically M was of the order of 600 frames. Note that $\vec{u}$ being a vector field, $\vec{\psi}$ must also be; however, we will also use the notation ψ when dealing with one component of the field (usually it will be the longitudinal component along x). A coherent structure can now be defined as an eigenmode of a (2-pointwise linear) correlation matrix built on the database snapshots. There exist mainly two ways of building up a correlation matrix: either performing a time correlation or a space correlation. With snapshots $\vec{u}(\vec{r},t)$ of size $N=N_x\times N_y$ pixels (where $N_x\simeq125$ and $N_y\simeq100$ are, respectively, the snapshot dimensions along x and y), the space-correlation matrix

$$\mathbf{K}(\vec{r},\vec{r}')=\int_0^{t_M}u_p(\vec{r},t)u_q(\vec{r}',t)dt$$

is of size $2N^2$ ($u_{p,q}$ are velocity components). We restricted our analysis to the x,y components of the velocity field so as to mimic what is available from 2D experimentalParticle Image Velocimetry (PIV) snapshots. On the contrary, the time-correlation matrix

$$\mathbf{C}(t,t') = \int\int_{S} \vec{u}(\vec{r},t)\vec{u}(\vec{r},t')d\vec{r}$$

is of size M^2, much smaller than $(2N)^2$ (3.6×10^4 versus 4×10^8). Keeping in mind that no more information can be extracted from that contained in the database itself, and that at most M relevant eigenmodes are therefore available from the data set, we chose the second way [based on $\mathbf{C}(t,t')$], known as the *snapshot* POD technique in the literature [4,9,10]. Practically, we start with a database of M instantaneous spatial snapshots of the velocity field; in experiments they can, for example, be obtained using PIV techniques [8]. Then, the data are reshaped into a "data matrix" $\mathbf{A}$ whose column elements are the pixels of a given snapshot. For that purpose, each 2D snapshot is reshaped into a column vector (of length N), by stacking over each other all the columns of the snapshot, from the first to the last. Both x and y components of the (vector) velocity field are further stacked in the same column following the same procedure, starting with component x at the top of the column, and then the component y, down to the bottom of the column. The vertical size of $\mathbf{A}$ is therefore $2N$. The matrix $\mathbf{A}$ contains as many columns as snapshots in the database (so that its horizontal dimension is M), the snapshots being ranked from the left to the right of A as the time is flowing down. The matrix $\mathbf{A}$ is therefore of dimension $M\times2N$. The correlation matrix $\mathbf{C}$ is next obtained by performing the product $\mathbf{C}=\mathbf{A}^t\cdot\mathbf{A}$, where $\mathbf{A}^t$ is the transposed matrix of $\mathbf{A}$, and $\cdot$ the usual matrix dot product. (Note that the space-correlation matrix $\mathbf{K}$ is given by $\mathbf{K}=\mathbf{A}\cdot\mathbf{A}^t$.) Applying a singular value decomposition procedure on $\mathbf{C}$, we obtain the eigenmodes $\phi_n(t)$, rearranged as columns of a *chronos* [10] matrix $\mathbf{\Phi}$ from left with $n=1$ to right with $n=M$. The spatial eigenmodes $\vec{\psi}_n(\vec{r})$ (sometimes called *topos* in the literature [10]) are given following Eq. (1) by $\vec{\psi}_n(\vec{r})=1/\mu_n\int\phi_n(t)\vec{u}(\vec{r},t)dt$. The $\vec{\psi}_n$ are reshaped into columns of a topos matrix $\mathbf{\Psi}=(\mathbf{A}\cdot\mathbf{\Phi})\cdot\mathbf{D}^{-1/2}$, following the same procedure as $\mathbf{A}$, where $\mathbf{D}$ is the diagonal matrix of the eigenvalues λ_n, ranked from the largest to the smallest value. The MATLAB© software is dedicated to matrix operations, so that the whole process of building $\mathbf{A}$, calculating $\mathbf{C}$, performing the singular decomposition to obtain the ϕ_n, and determining the ψ_n, takes, for $M=600$ and $N\simeq37\,300$, no more than 30 sec on a usual PC.

We first present in Fig. 1 the spectral distribution of time series provided by local recordings of one component of the velocity field [here the longitudinal component $u_x(t)$]. Velocity recordings are done at four different locations: two within the mixing layer (one upstream, one downstream), and two within the cavity (upstream and downstream). In each of them clearly appear peaks at about $f_0=13.5$ Hz (Strouhal number $St=1.06$ when based on the cavity length L and the reference velocity; $St=0.033$ when based on the mixing layer thickness and the mean velocity—to be compared with the natural Strouhal number $\mathrm{St}_n=0.03$ of an unforced mixing layer [2]), and it is now well accepted that this frequency is produced by the instability of the mixing layer [1]. The spectral component is recovered anywhere in the cavity, presumably due to the overall pressure field coupling due to the fluid incompressibility (the Mach number is about 4×10^{-3}).

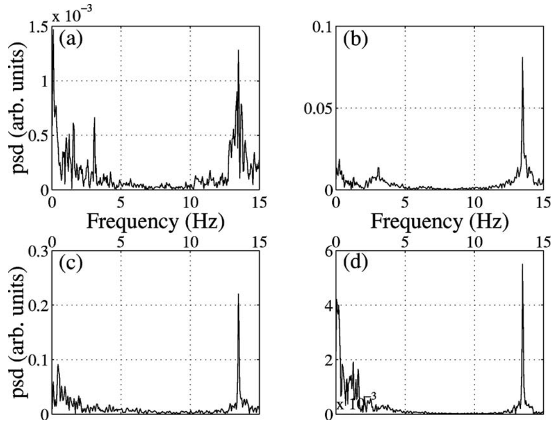

FIG. 1. Power spectral distribution of the x-component velocity time series collected in the mixing layer (a) upstream and (b) downstream, within the cavity, (c) upstream and (d) downstream, from 3D direct numerical simulations.

Now we propose to apply our technique so as to identify the spatial coherent structures $\vec{\psi}_n(\vec{r})$ of the flow fluctuations (with respect to the main velocity field), and track out their dynamical features from their associated time-dependent amplitudes $\phi_n(t)$. Note that the snapshots here must be sampled at least at $2f_0\simeq30$ Hz if we want to be time resolved with respect to f_0 (Shannon criterion). This was actually achieved in the numerical simulations.

In Fig. 2 we clearly see that the POD decomposes the flow into two well-defined areas: one is the mixing layer over the cavity, essentially captured by the two first eigenmodes $\psi_{1,2}$; the other is the cavity vortices, captured by the higher-order (less energetic) eigenmodes. The two first modes look very similar, and actually could be phase squared as expected when the flow is experiencing a global mean advection (phase squaring resulting in that case from the space translation invariance) [3]. However, when comparing the eigenvalues $\lambda_{1,2}$ plotted in Fig. 3(a), they appear to be rather different, and not close to each other, as should be expected in a phase squaring situation. Moreover, when plotting chronos $\phi_2(t)$ versus $\phi_1(t)$ [Fig. 3(b)], a torus is drawn whose dispersion cannot be explained by numerical noise. Henceforth, it rather looks like if the two first modes were not two degenerated phase aspects of a unique "complex" mode, but really two different POD modes, although somehow coupled [so as to produce the torus shape of Fig. 3(b)]. This invokes a symmetry breaking in the flow advection, most likely due to the downstream corner of the cavity. In the discussion on whether the instability is convective or absolute, note the downstream corner location of the two first topos $\vec{\psi}_{1,2}$, whose amplitude is vanishing in the upstream area. This is a strong argument in favor of the convective nature of the instability, the upstream front of the instability wave packet being expected to spread back against the flow advection in an absolutely unstable situation. A global mode cannot be completely excluded however [2].

In Fig. 4 are shown the five first time series $\phi_n(t)$ and their spectral distribution. We clearly see the occurrence of the frequency $f_0=13.5$ Hz associated with the two first chro-

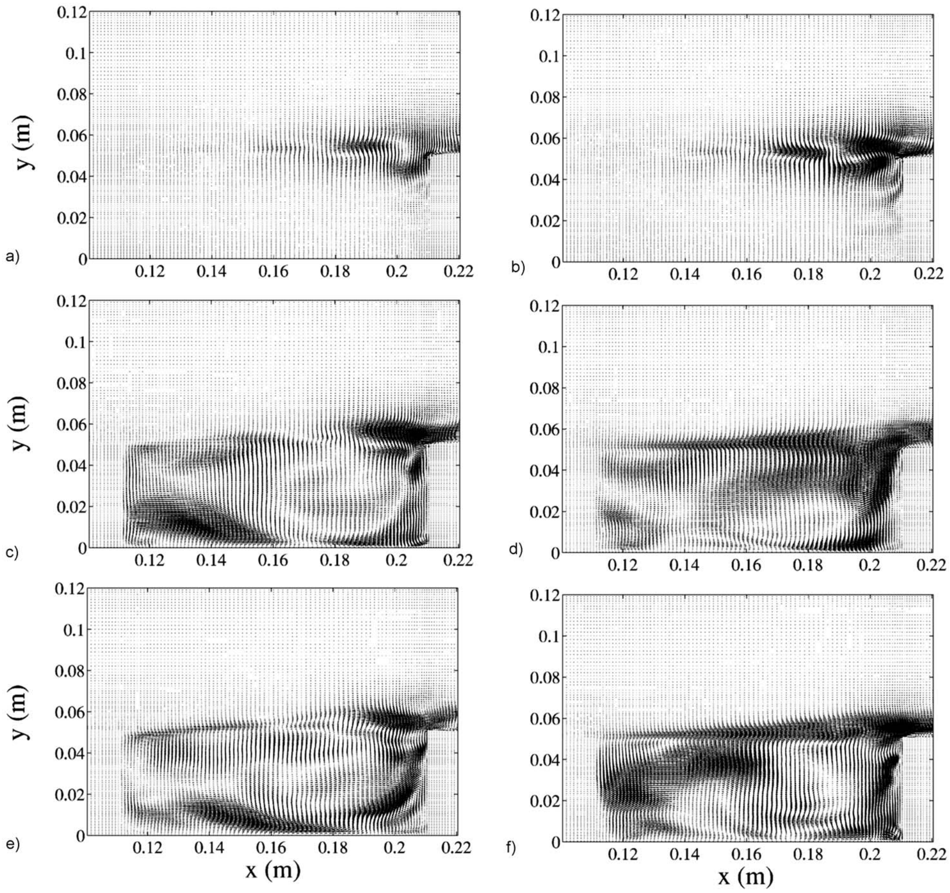

FIG. 2. The six first spatial eigenmodes [topos $\psi_n(\vec{r})$ with $n=1$ to 6 from (a) to (f)]. The arrows represent the velocity vector in the plane of the mode (here components x and y).

nos, the corresponding topos featuring the coherent structures contained in the mixing layer. Clearly, the frequency turns out to be associated with the instability that develops in the mixing layer. While local time series all produce spectral components at f_0 (see Fig. 1), the POD instead is able to overcome this global flow coherence and to selectively associate the spectral components to the adequate spatial coherent structures. This result henceforth naturally confirms the mixing layer origin of the most energetic spectral component.

At this step, it might be interesting to briefly discuss some critical points of the technique. First, because the method is aimed to track out coherent patterns encountered within a flow (coherent with respect to the pointwise correlation matrices), it is important for the statistical flow properties to be stationary. As a consequence, the data set must possess a sufficiently important number of independent realizations so

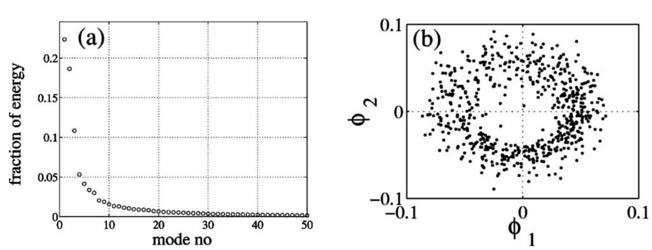

FIG. 3. (a) Singular value decomposition spectrum. Note the two first eigenvalues, which are not equal. (b) Phase portrait of $\phi_2(t)$ vs $\phi_1(t)$.

as to ensure the convergence of the decomposition towards the real POD modes. We have checked that for a data set of less than 400 samples, the third mode fairly mixes both shear layer and cavity structures, resulting in its time amplitude Fourier spectrum to the occurrence of the 13.5-Hz peak—strongly weakened here in mode 3 when using 600 samples. Secondly, from an experimental point of view, each sample composing the data set should share identical (statistical) properties; as a consequence, when directly working on instantaneous snapshots of the flow, particule feeding should remain homogeneous over time, the average intensity and coherent structure resolution being modified as the feeding is varying—therefore biasing the statistical representativity of the samples [8]. There are no systematic tests to decide whether statistical convergence has been reached or not. We, however, plotted in Fig. 5 the average difference η between two modes with respect to the data set number of snapshots,

$$\eta(p) = \frac{1}{N}\int_{\mathcal{S}} \big| |\psi_1^{p+1}(\mathbf{r})| - |\psi_1^{p}(\mathbf{r})| \big| d\mathbf{r},$$

where $\psi_n^p(\mathbf{r})$ is the nth topos computed using p snapshots in the data set for the single x component of the velocity. (Note: we had to deal with the absolute value of the topos to get rid of the sign, since cyclic global sign inversions from ψ_1^p to ψ_1^{p+1}, without deep modification of the velocity structure, were observed). Figure 5 suggests that convergence is ensured for mode 1 with $p \sim 400$ flow realizations.

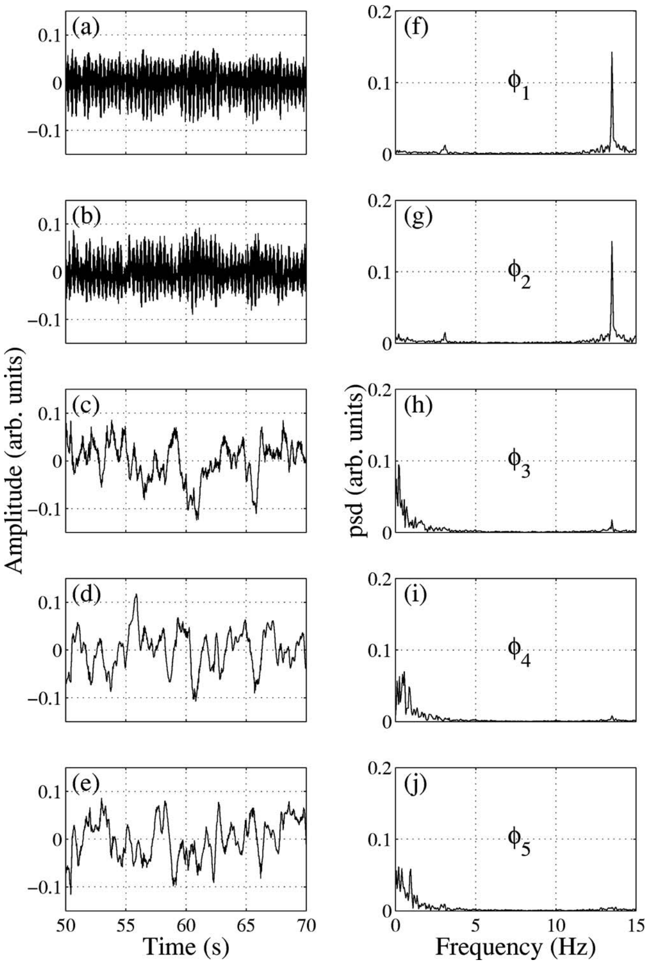

FIG. 4. From (a) to (e): five first time eigenmodes [chronos $\phi_n(t)$ with $n=1$ to 5]. From (f) to (j): associated eigenmode power spectral distributions.

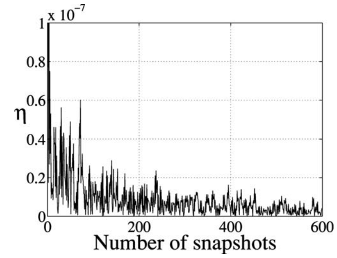

FIG. 5. Convergence test of mode 1 passing from p samples to $p+1$ in the data set. See text for a description of the η criterion.

The study reported here in fact brings another very interesting insight from an experimental point of view. It indeed shows that, although the velocity field is spatially fully 3D and characterized by three components [11], a 2D POD calculation (performed in a plane), over two velocity components, is able to separate the two intuitive regions of interest in the flow (namely the mixing layer and the cavity vortices), which therefore strongly simplifies any experimental protocol, in that a classical PIV (in a plane, over two velocity components) is sufficient to track out the coherent structures and their dynamical features, without having to call upon 3D PIV techniques. We have checked that the results were very similar when using 1 or 3 velocity components instead of 2. Moreover, the 3D calculation of the POD modes confirms all the results provided by the 2D analyses; 2D cuts out of the 3D modes look very similar to our (intrinsically) 2D modes, and their amplitude spectral distributions are comparable as well (see [11]).

In conclusion, a POD technique has been applied with success to discriminate the relevant dynamical features of the coherent structures present in the flow over an open cavity. The processing time revealed to be of the order of 30 s for about 600 samples of size 37 300 pixels, and grew up to 11 min when applied to about 300 experimental PIV samples of size 241.800 pixels ($N=260\times465$). However, in most experimental applications, the whole field resolution, or the whole picture area, is not required to get the expected results, and it is expected that the technique could efficiently be applied to a panel of other open flows presenting self-sustained oscillations.

MATLAB programs can be obtained from the authors upon request.

[1] D. Rockwell and E. Naudascher, Annu. Rev. Fluid Mech. **11**, 67 (1979); W. K. Blake and A. Powell, in *Recent Advances in Aeroacoustics*, edited by A. Krothapalli and A. C. Smith (Springer, Berlin, 1986) pp. 247–335.

[2] P. Huerre and M. Rossi, in *Hydrodynamics and Nonlinear Instabilities*, edited by C. Godrèche and P. Manneville (Cambridge University Press, Cambridge, England, 1998), pp. 81–294.

[3] P. Holmes, J. L. Lumley, and G. Berkooz, *Turbulence, Coherent Structures, Dynamical Systems and Symmetry* (Cambridge University Press, Cambridge, England, 1996).

[4] L. Cordier and J. P. Bonnet contribution to the VKI Lectures Series: Post Processing of Experimental and Numerical Data, Van Karman Institute editions, Feb. 17–21, 2003.

[5] M. Loève, Acad. Sci., Paris, C. R. **220**, 295 (1945); K. Karhunen, Ann. Acad. Sci. Fenn., Ser. A1: Math.-Phys. **34**, 7 (1946).

[6] F. Lusseyran *et al.*, in Proceedings of the 21st ICTAM, Varsaw, Poland, 2004 edited by W. Gutkowski and T. A. Kowalewski (Springer-Verlag, 2005), pp. 15–21.

[7] E. Gadouin, P. Le Quéré, and O. Daube, Int. J. Numer. Methods Fluids **37**, 175 (2001).

[8] Note that when dealing with PIV samples, the velocity field is always defined at each pixel of the picture, whatever the feeding is (this one just being important for the accuracy in the velocity estimation), so that most of the requirements may be fulfilled by the data samples.

[9] M. Kirby and L. Sirovich, IEEE Trans. Pattern Anal. Mach. Intell. **12**, 103 (1990).

[10] M. P. Chauve and P. Le Gal, Physica D **58**, 407 (1992).

[11] B. Podvin, Y. Fraigneau, F. Lusseyran, and P. Gougat, J. Fluids Eng. (to be published).